Published in final edited form as:
Invest Radiol. 2011 August ; 46(8): 509–514. doi:10.1097/RLI.0b013e3182183a95.

Noninvasive *in vivo* assessment of renal tissue elasticity during graded renal ischemia using MR Elastography

Lizette Warner, PhD[1], **Meng Yin, PhD**[2], **Kevin J. Glaser, PhD**[2], **John A. Woollard**[1], **Carolina A. Carrascal**[3], **Michael J. Korsmo**[1], **John A. Crane**[1], **Richard L. Ehman, MD**[2], and **Lilach O. Lerman, MD, PhD**[1]

[1]The Division of Nephrology and Hypertension, Department of Medicine, Mayo Clinic, Rochester, Minnesota, USA

[2]Department of Radiology, Mayo Clinic, Rochester, Minnesota, USA

[3]Department of Biomedical Engineering, Mayo Clinic, Rochester, Minnesota, USA

Abstract

Objectives—Magnetic Resonance Elastography (MRE) allows noninvasive assessment of tissue stiffness *in vivo*. Renal arterial stenosis (RAS), a narrowing of the renal artery, promotes irreversible tissue fibrosis that threatens kidney viability and may elevate tissue stiffness. However, kidney stiffness may also be affected by hemodynamic factors. This study tested the hypothesis that renal blood flow (RBF) is an important determinant of renal stiffness as measured by MRE.

Material and Methods—In six anesthetized pigs MRE studies were performed to determine cortical and medullary elasticity during acute graded decreases in RBF (by 20, 40, 60, 80, and 100% of baseline) achieved by a vascular occluder. Three sham-operated swine served as time control. Additional pigs were studied with MRE six weeks after induction of chronic unilateral RAS (n=6) or control (n=3). Kidney fibrosis was subsequently evaluated histologically by trichrome staining.

Results—During acute RAS the stenotic cortex stiffness decreased (from 7.4 ± 0.3 to 4.8 ± 0.6 kPa, p=0.02 vs. baseline) as RBF decreased. Furthermore, in pigs with chronic RAS (80±5.4% stenosis) in which RBF was decreased by 60±14% compared to controls, cortical stiffness was not significantly different from normal (7.4 ± 0.3 vs. 7.6 ± 0.3 kPa, p=0.3), despite histological evidence of renal tissue fibrosis.

Conclusion—Hemodynamic variables modulate kidney stiffness measured by MRE and may mask the presence of fibrosis. These results suggest that kidney turgor should be considered during interpretation of elasticity assessments.

Keywords

MR Elastography; MRI; kidney; stiffness

CORRESPONDING AUTHOR: Lilach O. Lerman, MD PhD Division of Nephrology & Hypertension Mayo Clinic 200 First Street SW Rochester, MN, 55905 USA Tel + 1 507 284 4695; Fax + 1 507 266 9316; lerman.lilach@mayo.edu.

Introduction

Renal disease often involves vascular and tissue remodeling (1). Renal arterial stenosis (RAS) is a narrowing of the renal artery that may induce chronic progressive renal disease, and is characterized by underperfusion of the kidney and tissue scarring emanating from tubulointerstitial fibrosis. In organs such as the liver, progression of fibrosis is associated with elevated tissue stiffness, which serves as an index of chronic hepatic remodeling (2). Similarly, renal fibrosis characterizes many forms of renal disease (3-5), and may be useful for monitoring renal disease progression or regression, because histopathologic damage is an important determinant and predictor of renal functional outcome (6). Currently renal biopsy is the best method to assess the severity of histopathological damage, but is invasive, susceptible to sampling errors, and impractical for longitudinal monitoring of treatment or renal disease progression. However, few techniques could assess the stiffness of the kidney *in vivo* and noninvasively.

A newly emerging diagnostic imaging technique, Magnetic Resonance Elastography (MRE), provides noninvasive assessment of tissue stiffness (7). MRE has been employed to assess myocardial stiffness (8) and shown to discriminate between moderate and severe fibrosis in chronic liver disease (2, 9, 10). Interestingly, patients with chronic liver disease, commonly associated with elevated portal hypertension, also have elevated splenic stiffness compared to normal volunteers (11), suggesting a potential hemodynamic contribution to tissue stiffness.

Indeed, changes in tissue stiffness as a result of hemodynamic variables, such as blood flow, may have considerable impact on *in vivo* elasticity measurements. For example, up to 25% of renal volume may be attributable to blood pressure and the content of blood, filtrate, and urine in the kidney, implying a substantial contribution of hemodynamics to renal turgor (12). However, the effects of hemodynamic alterations on assessments of kidney stiffness in vivo remain unknown. Therefore, this study was designed to test the hypothesis that changes in renal blood flow (RBF) affect the stiffness of the kidney as detected by MRE, independent of the presence of fibrosis. For this purpose pigs were studied with MRE during both acute unilateral reductions in RBF, as well as after six weeks of chronic unilateral RAS associated with renal fibrosis.

Materials and Methods

All animal experiments were reviewed and approved by the Institutional Animal Care and Use Committee. Eighteen domestic female pigs (48.9 ± 0.8 kg, Sus Scrofa, Manthei Hog Farm LLC, MN) were used for this study. For all studies, pigs were anesthetized (telazol 5 mg/kg and xylazine 2 mg/kg) and maintained with mechanical ventilation of 1-2% isoflurane in room air. An ear vein catheter was introduced for saline infusions (5 mL/min). A catheter (Cordis) was positioned in one carotid artery for monitoring mean arterial pressure (MAP).

Animal Models

For the acute RAS, both kidneys of six pigs were exposed through small flank incisions. A pneumatic inflatable vascular occluder was placed on one renal artery proximal to the renal artery bifurcation. MR compatible Doppler flow probes (Transonic System T206, probe 3RB429) were positioned on both renal arteries distal to the occluder for continuous monitoring of RBF. Incisions were closed and the animal prepared for imaging sessions. Renal volumetric scanning was performed prior to each of the six consecutive MRE studies in each pig, following a 5-minute rest period after establishing the progressive reduction in RBF by 20, 40, 60, 80 or 100 % of baseline in 15-minute intervals. A comparable sham-

operated group (n=3) was similarly prepared and underwent consecutive MRE studies without RBF alterations (Figure 1). After completion of all studies, the pigs were euthanized with sodium pentobarbital (100 mg/kg IV, Fort Dodge Laboratories).

For chronic RAS, six anesthetized pigs were similarly studied with MRE six weeks following the development of RAS induced by unilateral percutaneous implantation of a balloon-inflatable, local-irritant coil (Figure 1). A control sham-operated group (n=3) was similarly prepared except for coil implantation, and underwent similar consecutive MRE studies. Prior studies demonstrated development of a hemodynamically significant stenosis 5-7 days after implantation of the coil, accompanied by a significant decrease in stenotic kidney RBF, volume, and glomerular filtration rate (3, 13-15). Single-kidney RBF was measured in these pigs using multi-detector computed tomography (MDCT). After completion of studies, the pigs were allowed to recover for a few days (to allow for contrast media washout) and were subsequently euthanized with sodium pentobarbital.

Histology

Histology sections from the stenotic and contralateral kidneys were examined with a computer-aided image-analysis program (MetaMorph®, Meta Imaging Series 4.6, by JAW, who has 7 years of histology experience and was blinded to the degree of RAS). In each representative slide, immunostaining was quantified in 15-20 fields and expressed as percentage of staining of total surface area, and the results from all fields were averaged(16).

MRE Methods

After preparation, all animals were transported and positioned supine on a warming blanket in the MRI scanner, and blood pressure and heart rate monitored during the study. Imaging studies were performed after hemodynamic stabilization on a Signa EXCITE 3.0T system (GE Healthcare, Waukeshau, WI) using a 4-channel phased array coil. After localization, a renal volume series(17) was performed in the axial plane with a T2 weighted fast spin echo sequence using the following parameters: TR/TE/Flip angle/FOV /imaging matrix/thickness/ NEX = 2000ms/88 ms/90/35 cm/384×320×40/2.5mm/1.

MRE studies were performed using a spin-echo echo planar imaging sequence with flow compensation. Shear waves were induced by two cylindrical passive pneumatic drivers aligned along the posterior body wall. Continuous vibrations at 120 Hz generated shear waves throughout the abdominal tissues. Elastography data were collected with a spin echo EPI based MRE sequence with the following parameters: TR/TE/FOV /imaging matrix/ thickness/NEX/shots/ASSET factor = 2334ms/48 ms/35 cm/96×96×40/3mm/1/2/2, 4 phase offsets through one cycle of motion, 6 pairs of tetrahedral trapezoidal motion encoding gradients in 3 orthogonal directions with one motion encoding gradient on each side of the refocusing pulse synchronized with motion. Wave image pre-processing included two steps: phase unwrapping with minimum discontinuity; Gaussian bandpass filter with 8.75~35mm spatial cut-off (i.e. 10-40 waves/FOV) to remove undesired bulk motion in the background.

Multi-Detector Computed Tomography Methods

Two to 5 days following the MRE study, the chronic RAS and control animals were prepared for MDCT studies (Somatom Definition 64, Siemens Medical Solution, Forchheim, Germany) for noninvasive measurements of renal (cortical and medullary) volume and RBF (14, 15). In-vivo MDCT flow studies involved sequential acquisition of 160 consecutive scans after injection of iopamidol (0.5 mL/kg per 2 seconds) into a catheter positioned in the superior vena cava. A renal volume study was performed in the helical mode (5 mm thick slices) after a similar injection of contrast.

Following completion of the acute and chronic studies and after euthanasia, the kidneys were harvested, sectioned, preserved in paraffin, and stained with trichrome to assess fibrosis (18).

Image Analysis—Manually traced regions of interest (ROI) were selected in MRI (by CAC and MJK, with 2 years of image processing experience) or CT (LW, 4 years of experience) images in the renal cortex and medulla (14, 15, 19). Averages for the RAS groups were calculated from individual pig cortex and medulla ROI obtained in each stenotic or contralateral kidney. MRE analysis was performed (by CAC and MJK who had specialized training in processing MRE data and were blinded to the extent of stenosis) after typically placing 20 -30 ROIs in the medulla (52±9 mm^2) and cortex (149±26 mm^2). In the control groups ROI from both kidneys were compiled.

For the acute RAS studies, renal volume was computed semi-automatically from MRI images by blinded readers using the software package Analyze™ (Biomedical Imaging Resource, Mayo Clinic, Rochester, MN) using interactive auto-edge detection. Renal perfusion was assessed as the ratio of RBF to renal volume.

For elasticity, spatial displacement at different phases of the oscillation was measured, and stiffness maps (elastograms) obtained using the Helmholtz equation. Quantitative elastograms (20) and 3-dimensional stiffness maps of the kidneys (Figure 1A), were obtained with local frequency estimation inversion algorithm with 20 evenly spaced three dimensional directional filters (21) for the 3-D images. The elasticity was determined by averaging cortical or medullary elasticity obtained from the respective manually traced regions of interest on the elastograms.

In the chronic RAS group, RBF and GFR were assessed (LW, who was blinded to the degree of RAS) by tracing cortical and medullary ROI on the MDCT images using Analyze™, and analyzing time-attenuation curves using previously described methods (14, 15, 22). RBF was determined from the sum of the cortical and medullary RBF, the product of perfusion and volume. Renal volume was measured from CT images using planimentry with interactive edge-detection techniques. The degree of stenosis was assessed by renal angiography (JAC, a Medical Image Analyst with 5 years of experience).

Statistical Analysis

Comparisons within groups were performed by paired Student's *t*-test and among groups by analysis of variance (ANOVA), with post-hoc comparisons conducted with Tukey Kramer. Results are reported as mean ± SEM, and statistical significance was accepted for $p \leq 0.05$.

Results

All animals had similar body weight, and basal blood pressure was elevated only in the chronic RAS animals (Table 1). During an acute progressive stenosis, the stenotic kidney RBF, perfusion, and volume gradually decreased (Figure 2B-D). The contralateral kidney slightly increased its RBF, perfusion, and volume starting at 60% ipsilateral decrease in RBF, all of which achieved statistical significance by 100% decrease in RBF. An increase in mean arterial pressure (MAP) vs. control also reached statistical significance following 60% RBF decrease in acute RAS. RBF, perfusion, and volume of sham-operated control pigs remained unchanged throughout the experiment.

During the decrease in RBF, the stenotic cortical shear stiffness gradually decreased (Fig 3A), while the stenotic medullary stiffness decreased only at a total occlusion (100% stenosis) (Fig. 3B). Both contralateral and control cortical and medullary stiffness remained

unchanged throughout the experiment. The changes from baseline in the stenotic cortical RBF (ΔRBF) and stiffness (Δμ) during the acute stenosis were linearly related (r^2=0.85, p=0.03, Figure 3C) as: $\Delta\mu = 0.23\times \Delta RBF - 0.73$ (Eq. 1). Subsequent trichrome staining in kidneys excised from the acute RAS group was very similar to control levels (4.1±1.4 vs. 4.4±2.3% of renal surface area, p=0.9), ruling out development of fibrosis in the acute setting.

In the chronic RAS stenotic kidney (80±5.4% reduction in renal arterial diameter by angiography), RBF (Figure 4A) was lower than in the control and contralateral kidneys (−60±14%, p=0.03 vs. control). The shear stiffness of the stenotic cortex (Figure 4B) and medulla (Figure 4C) was similar to control values, but decreased compared to the contralateral kidney regions (p≤0.04 for both) that were significantly higher than control, as determined from the elastograms (Figure 4D). However, the stenotic cortex tended to have increased fibrosis compared to normal (16.6±8.4 vs. 1.5±0.6% of renal surface area, p=0.08) which has reached statistical significance in the contralateral kidney (5.9±1.5 vs. 1.5±0.6 %, p<0.04).

Discussion

The main finding of this study is that acute decreases in renal blood flow with no fibrosis lead to a decrease in renal cortical shear stiffness. Similarly, in chronic renal arterial stenosis the decrease in renal blood flow offsets a likely increase in stiffness secondary to development of renal fibrosis. Decreased renal stiffness may therefore mask the presence of renal fibrosis, but represent a marker of renal hypoperfusion.

Few techniques can assess tissue stiffness *in vivo* noninvasively. Diffusion weighted MR imaging potentially permits tracking fibrosis by measuring the restriction of water molecule motion, but lacks specificity for fibrosis. However, as this technique matures, standardization will likely correlate b-values with renal function making it a versatile and useful technique(23, 24). Emerging diagnostic imaging techniques such as ultrasound (25-28) or MRE offer assessment of tissue stiffness and are promising alternatives to invasive biopsies for assessing the progression of renal disease. Indeed, liver fibrosis has been demonstrated to be associated with elevated tissue stiffness (10, 11), and the MRE technique has been successfully employed clinically to assess hepatic fibrosis. Nevertheless, recent studies have observed that liver stiffness can increase secondary to acute liver damage, cardiac insufficiency, or increases in central venous pressure (29, 30), suggesting contribution of augmented hemodynamic factors to tissue stiffness (29, 31), which might complicate its utility as an index of fibrosis (31). Our study shows that in the kidney tissue stiffness can also drastically decline in conditions that decrease its arterial blood flow or perfusion pressure. Furthermore, changes in GFR and fluid reabsorption may also influence renal stiffness by virtue of intratubular fluid content and swelling.

Importantly, renal fibrosis is closely related to progression of kidney disease, and renal tissue injury is a major determinant of outcomes in chronic kidney disease (32). However, while renal biopsy is the reference standard for detection and quantification of histopathological damage, assessing the severity of renal injury non-invasively is challenging. With the advent of novel imaging techniques such as MR elastography, which offers *in vivo* assessment of the kidney stiffness non-invasively and longitudinally, it has substantial potential for monitoring kidney disease progression.

However, by examining alterations in kidney stiffness during hemodynamic perturbation in acute RAS, which is too brief to evoke detectable kidney fibrosis, the present study demonstrates that the stenotic kidney exhibits a RBF-dependent reduction in shear stiffness

in the cortex, which is independent of development of fibrosis. Furthermore, we confirmed this observation in chronic RAS kidneys that exhibited cortical shear stiffness similar to normal kidneys, despite the presence of fibrosis confirmed by histology. These observations suggest that hemodynamic factors are important determinants of renal cortical shear stiffness and may complicate detection of kidney fibrosis with techniques that rely on changes in tissue elasticity alone. Nevertheless, we cannot rule out the possibility that MRE is insensitive to small degrees of fibrosis. Moreover, in contrast to the cortex, medullary stiffness may have been far less prone to change with renal perfusion, possibly because its blood flow is less dependent on hydrostatic pressure (33), and because renal vascular resistance resides mainly in cortical microvessels, which contributes around 90% of RBF.

Notably, contralateral kidney stiffness increased only in chronic, but not in acute RAS. While this might be due to the greater increase in MAP observed in chronic RAS, it is possible that in acute RAS the kidney can eliminate some of the fluid volume by pressure natriuresis, which becomes less efficient in chronic renovascular hypertension. Moreover, development of fibrosis in the contralateral kidney in chronic RAS(18, 34), as it develops hypertensive injury, might have contributed to the increase in stiffness observed in this kidney.

Limitations

Measurements of RBF in the chronic and acute animals in this study were obtained using different methods (CT vs. Doppler) and under different experimental conditions (noninvasively vs. after abdominal surgery and isolation of renal arteries), and were therefore not compared directly. However, studies indicate that concurrently assessed CT and Doppler measurements of RBF are comparable (35). Furthermore, each group was compared to its own similarly studied control group and contralateral kidney. Our evaluation of the relative contributions of RBF and fibrosis to renal elasticity also neglects to account for the effects of perfusion pressure, glomerular filtration, diuresis, etc, on renal turgor. Furthermore, in contrast to acute RAS, chronic RAS is associated with chronic inflammation and vascular remodeling that might affect elasticity as well. It is also likely that longer duration of ischemia with greater degrees of renal fibrosis and shrinkage would eventually lead to an increase in renal stiffness. Indeed, it remains to be determined if MRE is sufficiently sensitive to detect small degrees of fibrosis.

In summary, Magnetic Resonance Elastography provides a noninvasive assessment of tissue stiffness, which is versatile, non-invasive, offers longitudinal monitoring of disease progression, and eliminates potential sampling error inherent to biopsies. However, we observed that renal elasticity is also strongly dependent upon hemodynamic variables. Changes in RBF or renal perfusion pressure may therefore offset development of fibrosis, unless the effect can be accounted-for. Further studies are needed to illustrate the relationship (which might be non-linear) between elasticity and fibrosis in a chronic setting and in humans, as well as the effects of hemodynamic perturbations on renal viscosity. Nevertheless, changes in renal turgor *per se* may represent a novel and surrogate measure of renal hemodynamic compromise which may shed light on the early detection and prevention of renal disease.

Acknowledgments

Funding Acknowledgement: Supported in part by NIH grants HL085307, EB001981, DK73608, HL77131, and DK73013.

References

1. Schlondorff DO. Overview of factors contributing to the pathophysiology of progressive renal disease. Kidney Int. 2008; 74:860–6. [PubMed: 18650795]
2. Rouviere O, Yin M, Dresner MA, et al. MR elastography of the liver: preliminary results. Radiology. 2006; 240:440–8. [PubMed: 16864671]
3. Chade AR, Zhu XY, Grande JP, et al. Simvastatin abates development of renal fibrosis in experimental renovascular disease. J Hypertens. 2008; 26:1651–60. [PubMed: 18622245]
4. Stephens SE, Rigden SP. Cystic fibrosis and renal disease. Paediatr Respir Rev. 2002; 3:135–8. [PubMed: 12297060]
5. Yiu WH, Pan CJ, Ruef RA, et al. Angiotensin mediates renal fibrosis in the nephropathy of glycogen storage disease type Ia. Kidney Int. 2008; 73:716–23. [PubMed: 18075499]
6. Keddis MT, Garovic VD, Bailey KR, et al. Ischaemic nephropathy secondary to atherosclerotic renal artery stenosis: clinical and histopathological correlates. Nephrology Dialysis Transplantation. 2010; 25:3615–22.
7. Elgeti T, Beling M, Hamm B, et al. Cardiac Magnetic Resonance Elastography: Toward the Diagnosis of Abnormal Myocardial Relaxation. Invest Radiol. 2010 Epub ahead of print.
8. Kolipaka A, McGee KP, Araoz PA, et al. MR elastography as a method for the assessment of myocardial stiffness: comparison with an established pressure-volume model in a left ventricular model of the heart. Magn Reson Med. 2009; 62:135–40. [PubMed: 19353657]
9. Elgeti T, Rump J, Hamhaber U, et al. Cardiac Magnetic Resonance Elastography: Initial Results. Investigative Radiology. 2008; 43:762–72. [PubMed: 18923255]
10. Yin M, Woollard J, Wang X, et al. Quantitative assessment of hepatic fibrosis in an animal model with magnetic resonance elastography. Magn Reson Med. 2007; 58:346–53. [PubMed: 17654577]
11. Talwalkar JA, Yin M, Venkatesh S, et al. Feasibility of in vivo MR elastographic splenic stiffness measurements in the assessment of portal hypertension. AJR Am J Roentgenol. 2009; 193:122–7. [PubMed: 19542403]
12. Lerman LO, Bentley MD, Bell MR, et al. Quantitation of the in vivo kidney volume with cine computed tomography. Invest Radiol. 1990; 25:1206–11. [PubMed: 2254054]
13. Chade AR, Rodriguez-Porcel M, Grande JP, et al. Distin.ct Renal Injury in Early Atherosclerosis and Renovascular Disease. Circulation. 2002; 106:1165–71. [PubMed: 12196346]
14. Chade AR, Zhu X, Lavi R, et al. Endothelial Progenitor Cells Restore Renal Function in Chronic Experimental Renovascular Disease. Circulation. 2009; 119:547–57. [PubMed: 19153272]
15. Daghini E, Primak AN, Chade AR, et al. Assessment of Renal Hemodynamics and Function in Pigs with 64-Section Multidetector CT: Comparison with Electron-Beam CT1. Radiology. 2007; 243:405–12. [PubMed: 17456868]
16. Zhu X-Y, Daghini E, Chade AR, et al. Simvastatin Prevents Coronary Microvascular Remodeling in Renovascular Hypertensive Pigs. J Am Soc Nephrol. 2007; 18:1209–17. [PubMed: 17344424]
17. Bakker J, Olree M, Kaatee R, et al. Renal Volume Measurements: Accuracy and Repeatability of US Compared with That of MR Imaging1. Radiology. 1999; 211:623–8. [PubMed: 10352583]
18. Lavi R, Zhu X-Y, Chade AR, et al. Simvastatin Decreases Endothelial Progenitor Cell Apoptosis in the Kidney of Hypertensive Hypercholesterolemic Pigs. Arterioscler Thromb Vasc Biol. 2010; 30:976–83. [PubMed: 20203299]
19. Warner L, Glockner JF, Woollard J, et al. Determinations of Renal Cortical and Medullary Oxygenation Using Blood Oxygen Level-Dependent Magnetic Resonance Imaging and Selective Diuretics. Investigative Radiology. 2011; 46:41–7. [PubMed: 20856128]
20. Yin M, Chen J, Glaser KJ, et al. Abdominal magnetic resonance elastography. Top Magn Reson Imaging. 2009; 20:79–87. [PubMed: 20010062]
21. Manduca A, Lake DS, Kruse SA, et al. Spatio-temporal directional filtering for improved inversion of MR elastography images. Med Image Anal. 2003; 7:465–73. [PubMed: 14561551]
22. Krier JD, Ritman EL, Bajzer Z, et al. Noninvasive measurement of concurrent single-kidney perfusion, glomerular filtration, and tubular function. American Journal of Physiology - Renal Physiology. 2001; 281:F630–F8. [PubMed: 11553509]

23. Carbone S, Gaggioli E, Ricci V, et al. Diffusion-weighted magnetic resonance imaging in the evaluation of renal function: a preliminary study. Radiol Med. 2008; 112:1201–10. [PubMed: 18074195]
24. Togao O, Doi S, Kuro-o M, et al. Assessment of Renal Fibrosis with Diffusion-weighted MR Imaging: Study with Murine Model of Unilateral Ureteral Obstruction. Radiology. 2010; 255:772–80. [PubMed: 20406881]
25. Pareek G, Wilkinson ER, Bharat S, et al. Elastographic measurements of in-vivo radiofrequency ablation lesions of the kidney. J Endourol. 2006; 20:959–64. [PubMed: 17144871]
26. Emelianov SY, Lubinski MA, Skovoroda AR, et al. Reconstructive ultrasound elasticity imaging for renal transplant diagnosis: kidney ex vivo results. Ultrason Imaging. 2000; 22:178–94. [PubMed: 11297150]
27. Arndt R, Schmidt S, Loddenkemper C, et al. Noninvasive evaluation of renal allograft fibrosis by transient elastography--a pilot study. Transpl Int. 2010; 23:871–7. [PubMed: 20158692]
28. Amador C, Urban MW, Warner LV, et al. In vitro renal cortex elasticity and viscosity measurements with Shearwave Dispersion Ultrasound Vibrometry (SDUV) on swine kidney. Conf Proc IEEE Eng Med Biol Soc. 2009; 2009:4428–31. [PubMed: 19963830]
29. Gunda M, Stefanie F, Stefanie A, et al. Liver stiffness is directly influenced by central venous pressure. Journal of Hepatology. 2010; 52:206–10. [PubMed: 20022130]
30. Sagir A, Erhardt A, Schmitt M, et al. Transient elastography is unreliable for detection of cirrhosis in patients with acute liver damage. Hepatology. 2008; 47:592–5. [PubMed: 18098325]
31. Lebray P, Varnous S, Charlotte F, et al. Liver stiffness is an unreliable marker of liver fibrosis in patients with cardiac insufficiency. Hepatology. 2008; 48:2089. [PubMed: 19003902]
32. Wright JR, Duggal A, Thomas R, et al. Clinicopathological correlation in biopsy-proven atherosclerotic nephropathy: implications for renal functional outcome in atherosclerotic renovascular disease. Nephrol Dial Transplant. 2001; 16:765–70. [PubMed: 11274271]
33. Jin C, Hu C, Polichnowski A, et al. Effects of Renal Perfusion Pressure on Renal Medullary Hydrogen Peroxide and Nitric Oxide Production. Hypertension. 2009; 53:1048–53. [PubMed: 19433780]
34. Lerman L, Textor SC. Pathophysiology of ischemic nephropathy. Urol Clin North Am. 2001; 28:793–803. [PubMed: 11791495]
35. Lerman LO, Schwartz RS, Grande JP, et al. Noninvasive Evaluation of a Novel Swine Model of Renal Artery Stenosis. J Am Soc Nephrol. 1999; 10:1455–65. [PubMed: 10405201]

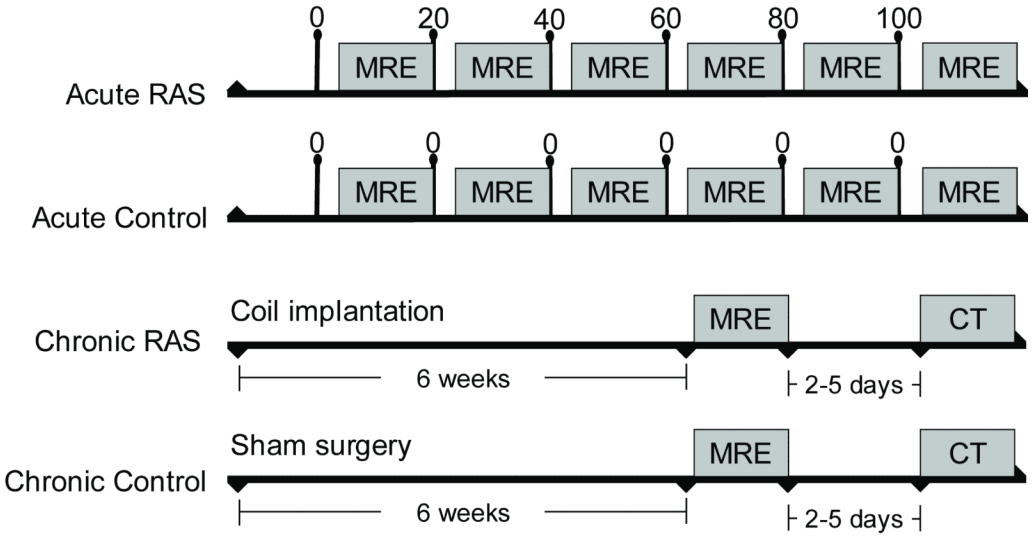

Figure 1.

Schematic of the experimental design for the acute and chronic studies. The acute experiment consisted of several periods in which renal blood flow (RBF), measured continuously by a flow probe, was decreased by 20,40,60, 80 and 100% of baseline, each followed by an MR elastography (MRE) study. In the Chronic RAS experiments, MRE and CT (RBF) studies were performed 6 weeks following development of RAS. RBF was not modulated in the control sham groups.

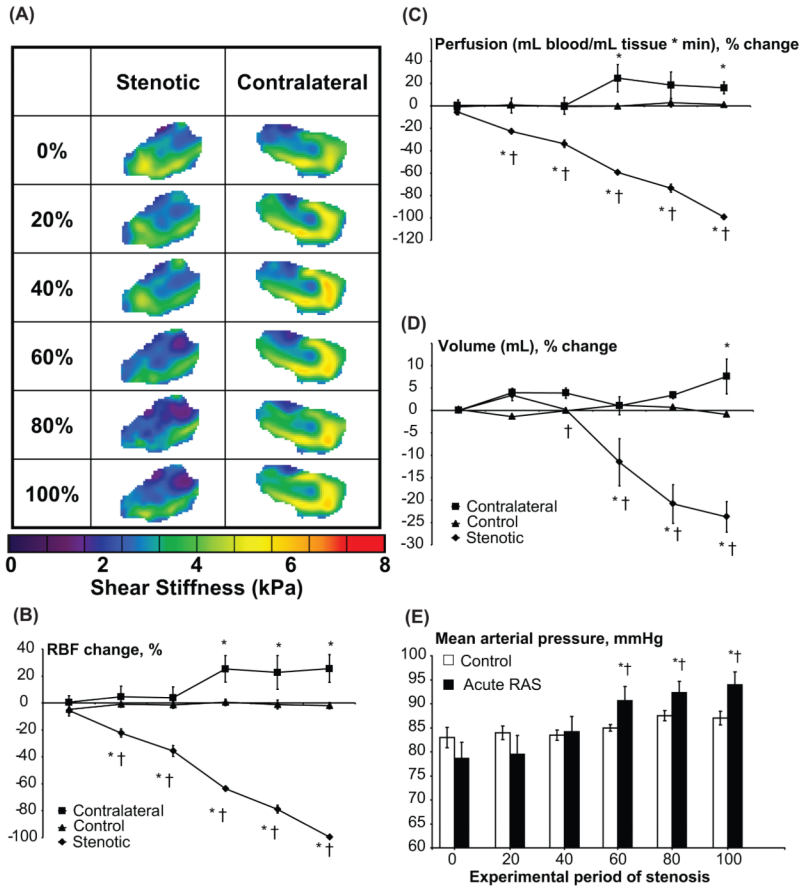

Figure 2.

Representative elastograms of the stenotic and contralateral kidneys (A). Right panel: renal blood flow (RBF, B), perfusion (C), and volume (D) of stenotic (solid diamonds), contralateral (solid squares), and sham-operated control (solid triangles) kidneys, and changes in blood pressure (D), during experimental decreases in RBF to 0,20,40,60,80 and 100% of baseline. * $p<0.05$ vs control, † $p<0.05$ vs contralateral kidney in the same period.

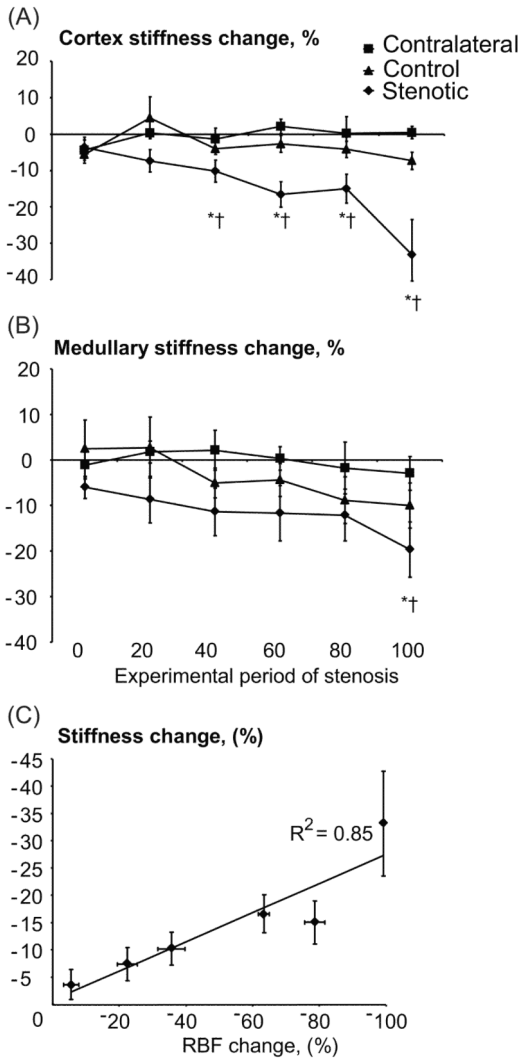

Figure 3.

Change in cortical (A) and medullary (B) stiffness of stenotic (diamonds), contralateral (squares), and sham-operated control (triangles) kidneys, and correlation between changes in cortical stiffness and renal blood flow (RBF, C), during acute graded decrements in RBF from baseline (0% stenosis). Tissue elasticity declined only in the stenotic kidneys.
* $p<0.05$ vs baseline (0 period), † $p<0.05$ vs contralateral kidney in the same period.

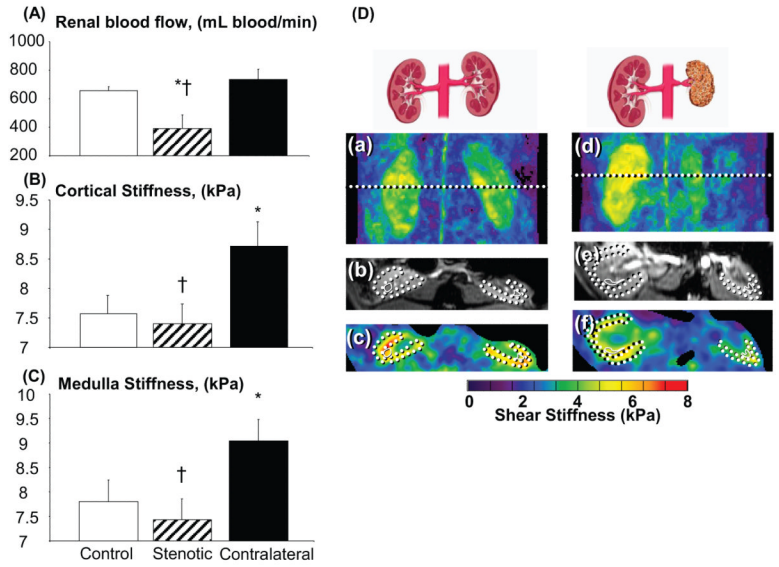

Figure 4.

Left panel: Renal blood flow (A), cortical (B), and medullary (C) stiffness in chronic experimental renal artery stenosis (RAS) and normal control kidneys. Right panel: Representative coronal elastograms (a, d), axial magnitude images (b, e), and axial elastograms (c, f) from control (a-c) and chronic RAS (d-f) animals, showing the stenotic and contralateral kidneys.

* $p<0.05$ vs control kidney, † $p<0.05$ vs contralateral kidney

Table 1

Baseline characteristics of the experimental groups

	Acute control	Acute RAS	Chronic control	Chronic RAS
Body Weight (kg)	50.3 ± 2.6	50.5 ± 1.5	49.4 ± 1.3	48.3 ± 1.3
Mean Arterial Pressure (mmHg)	84 ± 4	78 ± 2	83 ± 6	134 ± 11 *

RAS: renal artery stenosis.

* $p<0.05$ vs control group